JOURNAL OF MATERIALS SCIENCE 20 (1985) 4484–4496

Ultrasonic tests for phase separation in the vitreous systems Co–P–O and H–P–O

B. BRIDGE, A. A. HIGAZY*
Physics Department, Brunel University, Kingston Lane, Uxbridge, Middlesex, UK

Original data on ultrasonically determined elastic moduli of the vitreous systems Co–P–O and H–P–O have been used as a phase separation test for these glasses. For the Co–P–O system whose compositions ranged from 5 to 60 mol% CoO, no evidence for phase separation in any part of the composition range 0 to 42 mol% CoO could be found. The possibility of a narrow miscibility gap lying somewhere within the remaining composition range cannot be ruled out, though electron microscopy gave negative results. In the case of the H–P–O system whose compositions ranged from 0 to 50 mol% H_2O, the possibility of a miscibility gap somewhere within this range was indicated by the elastic moduli data. It would be well worthwhile to perform other kinds of phase separation tests on this system, though this will be difficult because of the rapidity with which water is absorbed. A qualitative theoretical interpretation of the results is attempted, from which it is concluded that the phase equilibrium of these phosphate glass sytems is determined by the vibrational energy and entropy at the melting temperature rather than the zero-point internal energy.

1. Introduction

Many oxide glasses consisting of more than one component have been shown to contain two-phase or multi-phase submicrostructures typically as small as 5 to 50 nm (for example K_2O–SiO_2, PbO–SiO_2, B_2O_3–GeO_3, SiO_2–GeO_2, PbO–GeO_2 and PbO–P_2O_5 glass systems). This phase separation results from liquid–liquid immiscibility which is widespread in glass-forming systems [1–5]. In recent reviews [6, 7] extensive bibliographies of attempts to describe the mechanism theoretically have been given. From the abundance of experimental results obtained to date concerning phase separation in glass, the following general propositions can be made on the most probable phase structures of oxide glasses:

(a) Melts consisting of a single component (for example SiO_2, P_2O_5, B_2O_3, GeO_2 etc), i.e. of a basic network former only, will, as a rule, solidify homogeneously.

(b) Melts whose compositions correspond to defined, stable chemical compounds (for example sodium metaphosphate), i.e. contain a single kind of structural element only, also solidify homogeneously.

(c) Melts consisting of two or more oxides whose compositions are intermediate between two stable compounds may tend to phase separation. The tendency is at least in part determined by the relative strengths and coordination numbers of the different types of bond present in the melt.

Most studies of phase separation in glasses (chiefly silicate and borosilicate glasses) have been made by means of electron microscopy. It is perhaps less well known that it is possible to perform a test for the presence or absence of two-phase systems ultrasonically, from an appropriate theoretical analysis of the compositional dependence of the elastic moduli found experimentally. The ultrasonic method,

Present address: Physics Department, Faculty of Science, Monofia University, Shebeen El-Kome, Egypt.

0022–2461/85 $03.00 + .12

although long, has certain advantages. For example it gives information on the interiors of bulk specimens whereas the electron microscope probes only the surface layers of bulk specimens, or thin sections by transmission. In hygroscopic glasses, like some phosphates for example, the surface structure has not the same structure as the rest of the specimen; layers rich in water may give indications on electron micrographs which obscure signs of phase separation, and the same problem may also arise with transmission sections. The ultrasonic method cannot by itself identify the presence or absence of multiphase systems. However, as will become apparent later, multi-phase oxide glasses are uncommon. In the usual case of miscibility gaps involving two phases only, whilst the absence of gaps can be established, their presence can be suggested but not proved. In spite of these limitations it seems well worthwhile to apply the ultrasonic technique to phosphate glasses, given the difficulties of performing electron microscopy on some compositional regimes of these systems. The method can possibly help, for example, in deciding which compositional ranges should be given priority for electron microscopy and other phase separation tests.

For the present study we had available original ultrasonic measurements of the elastic moduli of the entire vitreous range of the oxide systems Co–P–O and H–P–O. These measurements and the methods of preparation and chemical characterization of the glasses have been described elsewhere [8–11].

In earlier literature [12], binary P_2O_5 systems (involving potassium, sodium, lithium, barium, strontium, calcium, magnesium, beryllium, silver, tellurium, zinc, cadmium and PbO) have been considered to have continuous ranges of glass formation from pure P_2O_5 to the highest added oxide content, i.e. no regions of stable immiscibility were assumed to exist. However, microphase separation with droplet structure is observed in $MgO–P_2O_5$ glasses [12], and also P_2O_5 acts as a nucleating agent in precipitating phase separation in $Li_2O_2–SiO_2$ and Na_2SiO_2 glasses [13].

More recently [14], the possibility of phase separation in the $PbO–P_2O_5$ system has been proposed from an analysis of density data. So phase separation in phosphates remains very much an open question. The positive feature of the ultrasonic method to be described is that the absence of phase separation can be proved, whereas for phosphates one can never be 100% sure that phase separation is absent from electron microscopy alone.

2. General theoretical considerations of phase equilibrium in relation to ultrasonic tests

Phase separation is a thermodynamical phenomenon, i.e. under appropriate conditions a single phase splits into two or more phases if the free energy of the system is lowered in the process. According to Gibb's phase rule, for a binary glass (i.e. one independent component) only two phases can co-exist in equilibrium over a finite temperature range. The proposed ultrasonic test is thus applicable. For a ternary glass system (two independent components) up to three phases can co-exist in equilibrium over a temperature range, without violation of the phase rule. Interestingly, however, there appears to have been no direct observations of three-phase phenomena in ternary glass systems, although a three-phase region traversing the Vycor and Pyrex compositional range of the $Na_2O–B_2O_3–SiO_2$ system has been proposed on various grounds [15, 16]. Concerning glass systems with more components, no report of multi-phase separation exists amongst the extensive literature references presented here. As to the Co–P–O glass system under consideration here, at first sight (since it contains both Co^{2+} and Co^{3+} cations) it would be regarded as a ternary glass system with compositions $x\,CoO(x-y)Co_2O_3(1-x-y)P_2O_5$ where the values of the mole fractions x and y are given by the analysed amounts of $(Co^{2+} + Co^{3+})$, Co^{2+} and Co^{3+}, as presented in Fig. 1. However, it is clear that for a given x, y is fixed. In fact the relative values are determined by the redox equilibrium in the melts [10]. So there is only one independent variable specifying the composition and the glasses should be considered as a binary system. So in any event it is only possible for two phases to co-exist under the observation conditions and it is valid to apply the ultrasonc test.

For a binary system the simplest case of phase separation is when a single miscibility gap exists between two mole fractions C_1 and C_2 of one component. For mole fractions $C < C_1$ just a

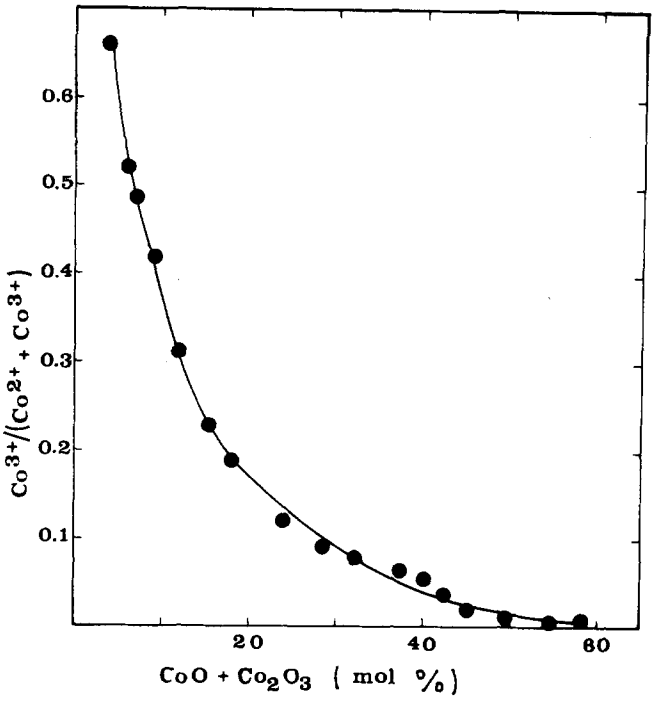

Figure 1 The chemical composition of Co–P–O glasses prepared by melting together Co_3O_4 and P_2O_5 in open crucibles according to the procedures described by Higazy and Bridge [10].

single phase (Phase 1) exists with composition continuously variable between 0 and C_1. Similarly for $C > C_2$ there exists but a single phase (Phase 2) with composition continuously variable between C_2 and some maximum value C_{max} which marks the end of the vitreous range. For $C_1 < C < C_2$, Phases 1 and 2 coexist with fixed compositions C_1 and C_2 respectively, and with relative proportions of $(C_2 - C_1)/(C_2 - C_1)$ and $(C - C_1)/(C_2 - C_1)$, respectively. In a more complicated case there may be two or more miscibility gaps and correspondingly a number of intermediate single-phase and two-phase regions. So essentially the ultrasonic test can only be successfully applied by considering all reasonable possibilities for the position and width of miscibility gaps in a binary glass system.

3. Theoretical considerations of the elastic behaviour of two-phase systems

So far, a number of investigators have considered theoretically the problem of expressing the bulk elastic behaviour of a two-phase material in terms of the amounts and properties of the end-member materials [17–21]. Generally, they discussed the upper and lower bounds between which the various elastic properties must lie.

Consider a binary system with a miscibility gap between weight fractions W_1 and W_2 of one of the components. Thus a material having weight fraction X ($X_1 < X < X_2$) of this component is a mixture of two phases with respective compositions X_1 and X_2, which we shall call the end-member components. Assuming that the volume of phase mixture is made up of the volumes of the constituent phases, the volume fraction of the second phase (composition X_2) in the material of composition X is related to the weight fractions and densities (ϱ_1 and ϱ_2) of the end-member components by

$$V_2 = \frac{\varrho_1(X - X_1)}{(X - X_1)(\varrho_1 - \varrho_2) + (X_2 - X_1)\varrho_2} \quad (1)$$

For binary material consisting of a matrix of volume fraction V_1 and a second phase of volume fraction V_2, the widest possible bounds can be found by assuming that the material is arranged in layers either parallel or perpendicular to an applied uniaxial stress. The first (Voigt) model assumes uniform strain; and the bulk modulus K^*, the shear modulus G^* and the

Young's modulus E^* of the composite become

$$K_U^* = (1 - V_2) K_1 + V_2 K_2 \quad (2)$$

$$G_U^* = (1 - V_2) G_1 + V_2 G_2 \quad (3)$$

$$E_U^* = (1 - V_2) E_1 + V_2 E_2 \quad (4)$$

where the subscripts 1 and 2 refer to the first and second end-member components.

The second (Reuss) model assumes uniform stress, and the moduli become

$$\frac{1}{K_L^*} = \frac{(1 - V_2)}{K_1} + \frac{V_2}{K_2} \quad (5)$$

$$\frac{1}{G_L^*} = \frac{(1 - V_2)}{G_1} + \frac{V_2}{G_2} \quad (6)$$

$$\frac{1}{E_L^*} = \frac{(1 - V_2)}{E_1} + \frac{V_2}{E_2} \quad (7)$$

Equations 2 to 4 form the upper limits and Equations 5 to 7 form the lower limits of the various quantities.

Evidently, one would expect the elastic moduli of a two-phase material to lie close to the Voigt and Reuss bounds only if the sample as a whole (i.e. the region over which the elastic moduli are measured) is rather anisotropic. A good example would be glass-fibre reinforced composites with oriented fibres. Hashin and Shtrikman [19] derived narrower upper and lower theoretical bounds for the moduli, for an arbitrary phase geometry subject only to the conditions that the sample as whole is isotropic and homogeneous. These conditions imply that one phase must consist of small particles and if the sample is divided up into smaller regions of equal volume τ, but still large compared with the particle size, the overall number, size and shape distribution of particles within each volume is the same. With this proviso the particles can have an arbitrary distribution of size and shape, possibly highly inhomogeneous on a microscopic scale. This is useful for it implies that the analysis will be valid for both the spinodal mechanism of phase separation (where one phase consists of multiple-connected filaments) and phase separation by the nucleation process. It is interesting to note also that subject to the above conditions of macroscopic isotropy and homogeneity, Hashin and Shtrikman [19] actually derived upper and lower bounds for the general case of a multi-phase material. However, for present purposes the argument of the preceding section implies that only the two-phase case is required.

Hashin and Shtrikman's expressions [19] were, for $K_2 > K_1$ and $G_1 > G_1$,

$$K_L^* = K_1 + \frac{V_2}{\frac{1}{K_2 - K_1} + \frac{3(1 - V_2)}{3K_1 + 4G_1}} \quad (8)$$

$$K_U^* = K_2 + \frac{1 - V_2}{\frac{1}{K_1 - K_2} + \frac{3V_2}{3K_2 + 4G_2}} \quad (9)$$

$$G_L^* = G_1 + \frac{V_2}{\frac{1}{G_2 - G_1} + \frac{6(K_1 + 2G_1)(1 - V_2)}{5G_1(3K_1 + 4G_1)}} \quad (10)$$

$$G_U^* = G_2 + \frac{1 - V_2}{\frac{1}{G_1 - G_2} + \frac{6(K_2 + 2G_2) V_2}{3G_2(3K_2 + 4G_2)}} \quad (11)$$

In these relations, K_U^* and G_U^* provide upper bounds, and K_L^* and G_L^* provide lower bounds on the respective moduli.

In the special case where one phase of volume fraction V_2 consists of spherical particles the lower bounds become exact expressions for the composite moduli, irrespective of the size distribution of the spheres. Analogously, the upper bounds become the exact result when the phase of volume fraction $(1 - V_2)$ consists of spherical particles, of arbitrary size distribution.

Values of Young's modulus were obtained by Hashin and Shtrikman [19] from the calculated bulk and shear moduli through the relation

$$E^* = \frac{9K^* G^*}{3K^* + G^*} \quad (12)$$

Upper and lower bounds on E are produced by inserting upper-bound or lower-bound values of K^* and G^*.

The slopes and curvatures of these relations shown in Equations 8 to 12 show that

(a) the slopes of the modulus–volume fraction curves depend only on the relative values of the end-member moduli;

(b) the curvatures of such plots are always positive, i.e. concave upward; and

(c) no maxima, minima or points of inflection or discontinuities can exist.

TABLE I Curvature of Hashin–Shtrikman/Kerner elastic moduli† (after Shaw and Uhlmann [17]). Weight per cent composition plots; ϱ denotes density, σ denotes Poisson's ratio.

Effective bulk modulus, K^*	Curvature	Effective shear modulus, G^*
$K_2 > K_1$ $\quad \frac{\varrho_1}{\varrho_2} < \frac{3K_2 + 4G_1}{3K_1 + 4G_1}$	Positive	$G_2 > G_1$ $\quad \frac{\varrho_1}{\varrho_2} < \frac{G_1(7 - 5\sigma_1) + G_2(8 - 10\sigma_1)}{G_1(15 - 15\sigma_1)}$
$K_2 < K_1$ $\quad \frac{\varrho_1}{\varrho_2} > \frac{3K_2 + 4G_1}{3K_1 + 4G_1}$		$G_2 < G_1$ $\quad \frac{\varrho_1}{\varrho_2} > \frac{G_1(7 - 5\sigma_1) + G_2(8 - 10\sigma_1)}{G_1(15 - 15\sigma_1)}$
$K_2 > K_1$ $\quad \frac{\varrho_1}{\varrho_2} > \frac{3K_2 + 4G_1}{3K_1 + 4G_1}$	Negative	$G_2 > G_1$ $\quad \frac{\varrho_1}{\varrho_2} > \frac{G_1(7 - 5\sigma_1) + G_2(8 - 10\sigma_1)}{G_1(15 - 15\sigma_1)}$
$K_2 < K_1$ $\quad \frac{\varrho_1}{\varrho_2} < \frac{3K_2 + 4G_1}{3K_1 + 4G_1}$		$G_2 < G_1$ $\quad \frac{\varrho_1}{\varrho_2} < \frac{G_1(7 - 5\sigma_1) + G_2(8 - 10\sigma_1)}{G_1(15 - 15\sigma_1)}$
$K_2 = K_1$ or $\frac{\varrho_1}{\varrho_2} = \frac{3K_2 + 4G_1}{3K_1 + 4G_1}$	Zero	$G_2 = G_1$ or $\frac{\varrho_1}{\varrho_2} = \frac{G_1(7 - 5\sigma_1) + G_2(8 - 10\sigma_1)}{G_1(15 - 5\sigma_1)}$

† The effective Young's modulus E^* will have the same curvature as the bulk and shear moduli over the same composition range. It should be noted that the shear modulus relations are quite insensitive to variations in Poisson's ratio. For example, variations in the effective shear moduli of less than one per cent result from changing σ from 0.2 to 0.3.

When elastic moduli are plotted as a function of the weight fraction X of one of the binary components (a) and (c) remain unchanged, but Shaw and Uhlmann [17] deduced that both positive and negative curvatures can be obtained according to the criteria summarized in Table I. We include this table because curvature can be a very useful parameter to use in phase separation tests, given that curvatures can be discerned even when there is a considerable spread in the experimental data.

4. The validity of comparing Hashin and Shtrikman formulae with ultrasonically determined elastic moduli of glasses

It is important to emphasize that the moduli derived by Hashin and Shtrikman [19] refer to static stress and strain distributions. However, ultrasonically applied stress and strain distributions exhibit cyclic variations across the sample in the direction of the wave propagation, at any instant of time. Ultrasonically one measures bulk and shear modulus from the equations

$$K + \tfrac{4}{3}G = \varrho C_L^2 \qquad G = \varrho C_T^2 \quad (13)$$

where ϱ is the density, C_L is the compressional wave velocity and C_T is the shear wave velocity, each quantity being a spatial average over the bulk sample. Consider the sample divided into layers parallel to the plane wave fronts, and of thickness Δx in the propagation direction. If $\Delta x \ll \lambda$ (the ultrasonic wavelength) the total distributed stress over the two faces of any layer will be almost the same, at any instant. If at the same time the values of C_L, C_T and ϱ averaged over each layer are the same, the moduli calculated from Equation 13 will be comparable with the static analysis of Hashin and Shtrikman [19]. It is clear that these conditions can only be met if the overall number, size and shape distribution of the particles of one phase is the same in all layers. A minimum requirement for this to be the case is that the mean particle size be $\ll x$ and therefore $\ll \lambda$.

For typical measurement frequencies (15 MHz) and wave velocities (4000 m sec^{-1}), the wavelength in oxide glass is ~ 0.3 mm. Since two-phase microstructures smaller than 0.05 μm are expected in multi-phase glass, the required condition seems to be easily met. If it could not have been met, ultrasonic wave velocities and the corresponding ultrasonically determined elastic moduli would have become sensitive functions of particle size relative to the wavelength [22, 23] and the Hashin and Shtrikman analysis could not then be applied.

Secondly, it will be appreciated that some composite materials can contain areas of debonding between the two phases of interest, i.e. there can arise air-filled or more generally fluid-filled gaps betwen them. Even though these gaps are invariably extremely small on the scale of the particle size, it is possible that they invalidate the boundary conditions assumed in Hashin and Shtrikman's derivation. When elastic moduli are measured ultrasonically rather than quasi-statically, there is the added complication

that the wave propagation properties depend upon the width of the gaps relative to the wavelength, i.e. the effect of the gaps on the measured modulus becomes frequency-dependent. This problem should not arise in the case of glasses in which particle sizes and separations are expected to be much less than the wavelength, and correspondingly the gaps between the solid phases will be even smaller.

5. Application to cobalt–phosphate glasses

Fig. 2 illustrates schematically the form of the compositional dependence of all the elastic moduli of the Co–P–O system throughout the entire vitreous range, 0 to 60 mol % CoO (43 wt %). Inspection of this curve in the light of Criterion (c) (Section 3) suggests immediately that there can be no two-phase immiscibility gaps traversing compositions 8 and 32 wt %. The next stage is to look for possible gaps in between or to either side of these regions, i.e. we refer to the ranges 3.4 to 8.2 wt %, 8.2 to 32.4 wt % and 32.4 to 43.0 wt %. The reason for quoting several significant figures here is that we refer to the analysed compositions of actual glass samples. The lowest figure gives the composition of the prepared Co–P–O glass having the smallest quantity of cobalt. We were unable to prepare glasses of compositions 0 to 3.4 wt % CoO [8]. Two-phase structures within these three ranges cannot be ruled out by visual

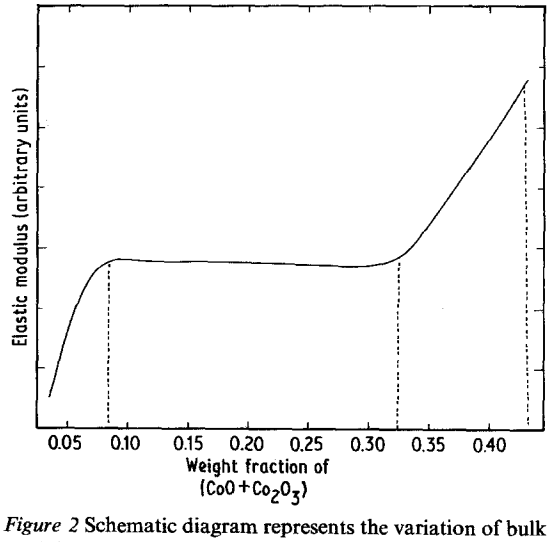

Figure 2 Schematic diagram represents the variation of bulk modulus with composition (weight fraction) of Co–P–O glasses.

inspection of Fig. 1, so more detailed tests in the form of a full application of Equations 2 to 12, together with a plot of experimental data on a larger scale than that of Fig. 1, are required. Taking the two ends of each range as the end-members in these equations, the variation in volume fractions being calculated from Equation 3, the variations of the theoretical bounds of each modulus with weight fraction of ($CoO + Co_2O_3$) are drawn in Fig. 3, which also indicates the experimental data points.

Examination of the figures shows that there is no evidence for two-phase immiscibility gaps covering these three compositional ranges in the Co–P–O glasses. This is because all experimental values of bulk, shear and Young's moduli lie well outside the upper and lower bounds of the K^*, G^* and E^* moduli. One can next seek narrower miscibility gaps within these ranges by bringing the end-members in the theoretical plots closer together.

To obtain a set of different H–S plots with variable end-member separations is clearly an unsatisfactory time-consuming procedure. Moreover, if we make the separations much smaller than the ones already considered the number of experimental data will be too small to permit a useful discussion. It is simpler instead to analyse the curvatures obtained in present plots. Now consider one or both the end-members to be moved inwards from the extreme values already discussed. Since experimental modulus and density values (Fig. 4) vary gradually from the values obtained at the composition extremes already discussed, it is obvious that the curvatures of the H–S plots will vary only gradually from the values displayed in Fig. 3.

When the curvatures displayed in these plots are pronounced it is unlikely that there will be a change in sign on moving together the end-members. Now for the ranges 3.4 to 8.2 wt % and 8.2 to 32.4 wt % the H–S curvatures and the experimental modulus plots have pronounced curvatures of the opposite sign. We conclude that it is unlikely that there is a miscibility gap of any size within these compositional ranges. Coming to the range 32.4 to 43.0 wt %, the curvature of both the H–S and the experimental modulus plots are of the same sign and of similar magnitudes. So we will not rule out the possibility of a narrow immiscibility gap within this range, from the ultrasonic data; and for these

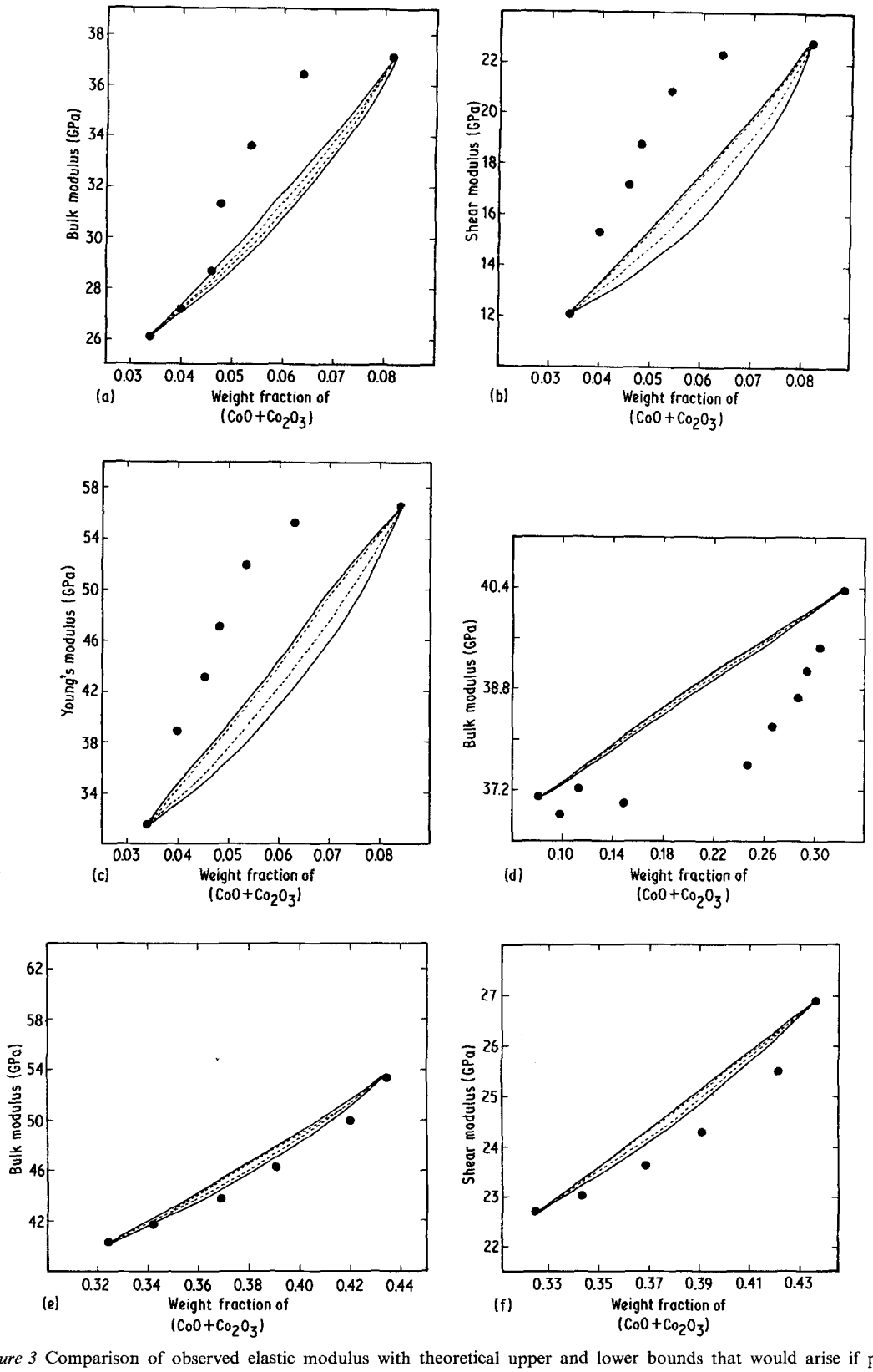

Figure 3 Comparison of observed elastic modulus with theoretical upper and lower bounds that would arise if phase separation is present, for Co–P–O glasses. Full circles represent the experimental data, solid lines show Voigt and Reuss boundaries, and dashed lines represent Hashin and Shtrikman [19] boundaries, with various assumed miscibility gaps.

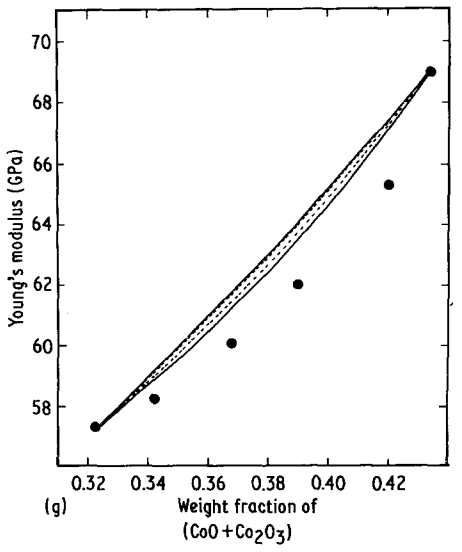

Figure 3 Continued.

high cobalt contents it is particularly tempting to suppose that the glasses might consist of mixtures of two amorphous phases of approximately metaphosphate and orthophosphate compositions.

Further investigation of possible phase separation phenomena in the Co–P–O glass system was made using electron microscopy. The investigations were based on the plastic replica technique, in which glass specimens were fractured. A plastic replica of a fractured glass surface was made using an acetate film softened by immersion in acetone for about 5 sec. When the acetate film was dry it was removed from the surface and shadowed with germanium and the carbon support film evaporated on to it using a coating unit. The plastic film was then removed, using solvent vapour, and the shadowed carbon replica supported on a grid ready for examination using a JEOL JEM–7 100 kV transmission electron microscope.

Replica electron micrographs of Co–P–O glasses showed no evidence that immiscibility is present in Co–P–O glass, so there is reasonable agreement between electron micrograph observations and the predictions of the above models, i.e. the ultrasonically determined elastic modulus tests. Transmission electron microscopy, requiring thin glass samples, was not attempted, as it was felt that water absorption would render all results unreliable.

6. Application to H_2O–P_2O_5 glasses

In the case of H_2O–P_2O_5 glasses, to perform a test for the possibility of two-phase behaviour within the compositional range of this system ultrasonically, two compositional regions were chosen. The first region lies between 0 to 11 wt % (50 mol % H_2O), and the second region from 0 to 100 wt % H_2O. The variation of experimental and predicted values of bulk, shear and Young's moduli with weight fraction of H_2O are plotted in Fig. 5.

It is seen from Figs. 5a and b (using HPO_3 and P_2O_5 as two end-members) that the experimental elastic modulus data of G and E lie between the upper and lower bounds of the Hashin–Shtrikman boundary in the glass compositional range between 3 and 11 wt % H_2O. Also in Fig. 5d (when H_2O and P_2O_5 are used as two end-members) the experimental bulk modulus data lie between the upper and lower bounds of K^* in the same compositional range (3 to 11 wt % H_2O) and lie only just outside the lower bound for the remaining composition range. And in both cases we note that the H–S plots and the experimental moduli have the same sign and a

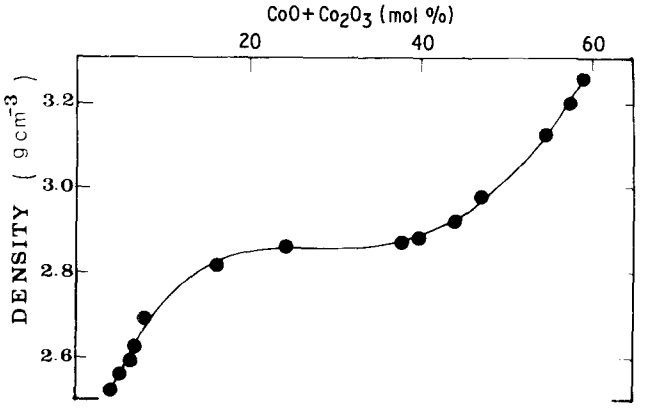

Figure 4 Compositional dependence of Co–P–O glass densities.

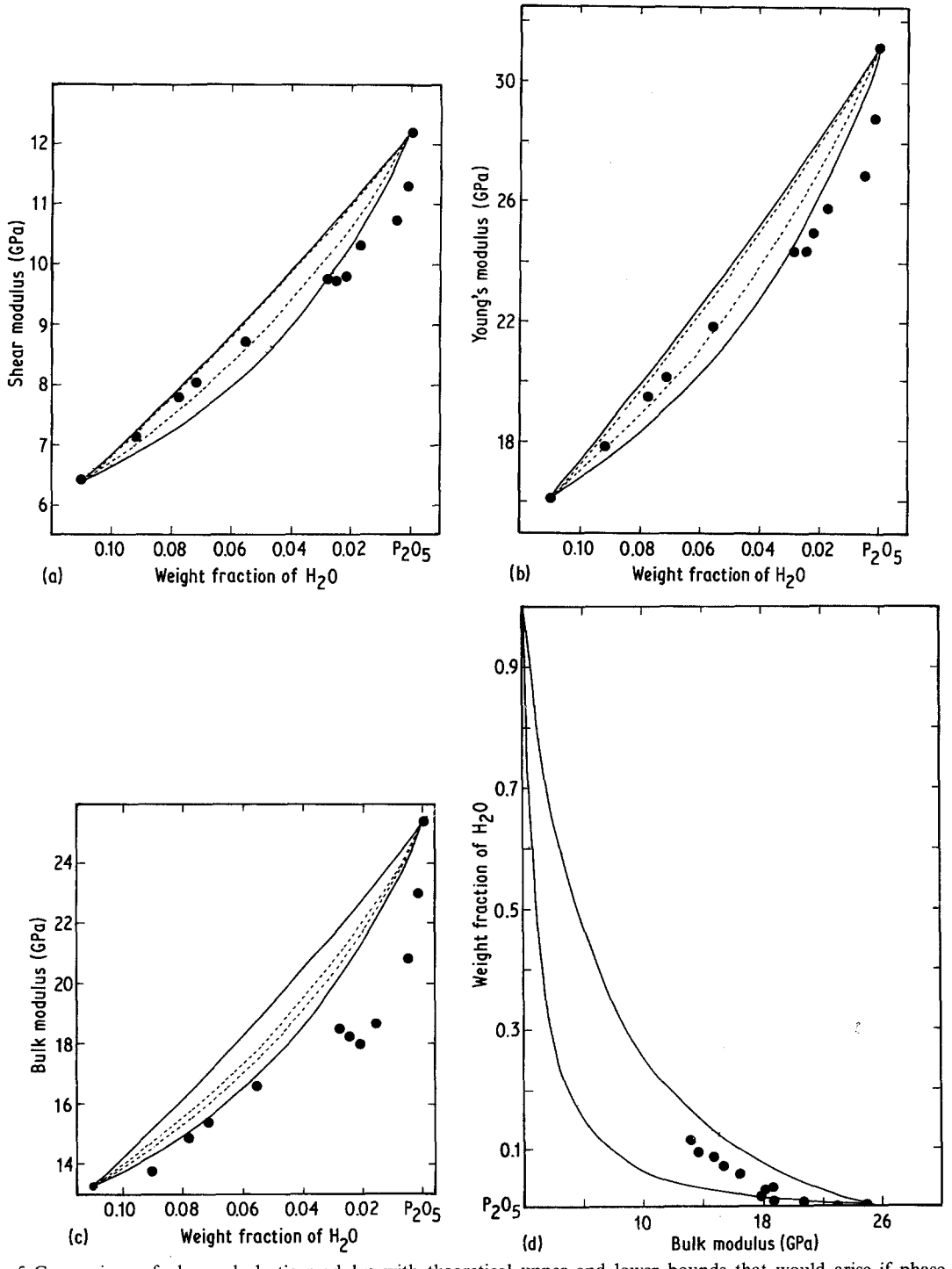

Figure 5 Comparison of observed elastic modulus with theoretical upper and lower bounds that would arise if phase separation is present, for H_2O–P_2O_5 glasses. Full circles represent the experimental data, solid lines show Voigt and Reuss boundaries, and dashed lines represent Hashin and Shtrikman boundaries, for various assumed miscibility gaps.

similar magnitude of curvature. The conclusion must be that phase separation in the H_2O–P_2O_5 system is a possibility. All samples of glass absorbed surface water too rapidly to make electron microscopy practicable.

7. Discussion and qualitative theoretical interpretation of results

It seems worthwhile to attempt to compare results with what might be expected theoretically

from available data on the glass systems. In a binary oxide glass containing two types of cation in one homogeneous phase, one can identify two basic kinds of bond, indicated by subscripts i ($i = 1, 2, \ldots$) and j ($j = 1, 2, \ldots$). The i bonds are associated with oxygen atoms which are shared between identical cations or which are bonded to only one cation (for example P=O bonds) while the j bonds are associated with oxygen atoms shared between different cations. Let n denote the number of bonds per cation of energy V, where V is negative and $|V|$ is the bond dissociation energy at absolute zero. Further let N and N^1 be the number of cations which are joined to the same cation or a different cation through a common oxygen atom, respectively. The Helmoltz free energy of the glass is

$$F = N \sum_i n_i V_i + N^1 \sum_j n_j V_j - \int_0^T \left[\int_0^T (C_p/T)\, dT \right] dT - T S(c) \quad (14)$$

where the summation terms contain the zero-point internal energy, C_p is the heat capacity, the integral term contains the vibrational internal energy and entropy, and $S(c)$ is the entropy of mixing. The Σ_i term essentially varies monotonically with c, so at $T \to 0$ K, only the magnitude of the Σ_j terms can cause the energy of the glass to be higher or lower than the unmixed oxides. If the former is the case the glass is unstable and tends to split into the two separate oxides, i.e. F has two minima at $c = 0$ and $c = 1$ respectively. On general statistical grounds it is accepted that $S(c)$ exhibits a single minimum at some intermediate value of c. So the effect of this term is always to shift the minima in F inwards to mole fractions $C_1 > 0$ and $C_2 < 1$. As T increases the miscibility gap $C_1 - C_2$ therefore decreases progressively, until a single minimum (implying no phase separation) is obtained above a temperature T_c (the upper consulate temperature).

As for the C_p term, since in general terms the contribution to C_p of a given bond increases with decreasing vibrational frequency ν, and ν decreases with increasing V, C_p increases with increasing V (i.e. decreasing $|V|$). So compositional gradients in C_p are of the same sign as compositional gradients in zero-point energy, and the negative sign in front of C_p thus implies that compositional gradients of the vibrational free energy oppose those of the zero-point energy. So, for example, a maximum in the free energy at low temperatures is depressed with increasing temperature and eventually becomes a minimum at sufficiently high temperatures, i.e. on account of the vibrational term a phase separation, impossible at low temperatures, may become possible at elevated temperatures. However, at ordinary temperatures oxide glass melts are regarded as network liquids, i.e. only a small fraction of bonds are ruptured so that the vibrational energy is expected to be small compared with the zero-point term. Ordinarily, therefore, we expect the effect of the vibrational term to be small so that valid conclusions can be reached by examination of the zero-point term alone.

According to the zero-point term, since $(N + N^1)$ is a constant for a given glass composition, the condition favouring separation into separate oxide phases is

$$\sum_j n_j V_j > \sum_i n_i V_i \quad (15)$$

which, since V is negative, can be alternatively written

$$\sum_j n_j |V_j| < \sum_i n_i |V_i| \quad (16)$$

This relation can be applied qualitatively to binary glasses by making the following assumptions:

(a) It is generally accepted [24] that for a bond between a given pair of atoms, the strength $|V|$ decreases as the length increases.

(b) For such a bond the length and therefore the strength varies relatively little from one structural grouping to another.

(c) In the absence of direct information (for example from extended X-ray absorption fine structure measurements), it is assumed that coordination numbers in a single glass phase resemble those obtaining in crystalline analogues (i.e. crystals of comparable composition), when they exist.

In the present discussion we have therefore drawn on bond lengths and coordination numbers already known for the crystal structure of P_2O_5 [25], cobalt metaphosphate ($Co(PO_3)_2$) [26, 27], cobalt pyrophosphate ($Co_2P_2O_7$) [28], CoO [29–31], and metaphosphoric acid (HPO_3) [11, 28, 32]. Data on oxides containing the Co^{3+} ion have been ignored but we consider it unlikely

that the small proportion of this ion in our glasses has a bearing on phase separtion.

7.1. Application to Co–P–O glasses

The P–O bond length changes relatively little between the different structural groups, being 0.156, 0.1543 and 0.1534 nm in P_2O_5, metaphosphate and pyrophosphate respectively. Also the phosphorus coordination remains tetrahedral throughout, so the presence or absence of phase separation rests with the P=O and Co–O bonds. In CoO which has the fcc structure of NaCl, the cobalt has octahedral coordination and a bond length of 0.21 nm. However, in vitreous cobalt metaphosphate (composition $CoO \cdot P_2O_5$) the cobalt coordination is reduced to tetrahedral [27] while the mean bond length is increased to 0.233 nm [26]*. Both factors act together to depress the value of $\Sigma n_j |V_j|$ relative to $\Sigma n_i |V_i|$, thus to favour phase separation into the constituent oxides. A similar conclusion would be reached if we considered the cobalt-rich phase in a phase separation model to resemble pyrophosphate (the composition of which approximates to the upper limit of the vitreous range found) rather than CoO, since the former has almost the same mean Co–O bond length (0.2083 nm) and the same cobalt coordination as the latter. Concerning the P=O bond, the infrared spectra of these glasses [9] suggest that this bond is progressively ruptured with increasing cobalt content, to be replaced by P–O–Co bridging units. Now the P=O bond dissociation energy for P_4O_{10} (156 k cal mol^{-1}) is almost twice the P–O energy (80 k cal mol^{-1}). This presents an even greater contribution to the reduction of $\Sigma n_j |V_j|$ than the previously discussed reduction in cobalt coordination number, and strongly favours phase separation and suggests that the P=O bond ruptures indicated by the infrared spectra should not take place. Indeed one could argue that to compensate for the effect of the P=O bond rupture thus to make the single phase favourable, the cobalt coordination would have to be doubled to sixteen, which is unknown in any cobalt compound.

Since experimentally from ultrasonic and electron microscope evidence (Fig. 6) a single phase has been found, at least for compositions below 50 mol % CoO, we can only conclude that the vibrational energy and entropy in the melt must be responsible for the formation of a single phase. It is certainly known that binary phosphate glasses exhibit unusual vibrational behaviour, inasmuch as in a given system, some compositions exhibit strongly anomalous third-order elastic constants (TOEC) whilst others display normal TOEC [33]. Moreover a strong maximum in the composition dependence of the thermal expansion coefficients in Co–P–O glasses has been observed at the metaphosphate composition [27]. It is thus clear that the vibrational modes in phosphate glass exhibit a singular composition dependence, and so therefore will C_p.

7.2. Application to H_2O–P_2O_5 glasses

We shall assume that a single phase consisting of 50 mol % H_2O will have a structure resembling metaphosphoric acid (HPO_3), in so far as the P–O bond lengths are concerned. This length is 0.14 nm [27, 32], substantially less than in P_2O_5. We conclude that the formation of metaphosphate groupings leads to a substantial contribution to $\Sigma n_j V_j$ from the P–O bonds (coordination number assumed unchanged.) We shall assume that the energies associated with the P=O bond remain the same in P_2O_5 and HPO_3, and likewise for the OH group in water and HPO_3. Thus the only remaining consideration is the energies of the hydrogen bonds in water and in metaphosphate. Patel *et al.* [11] have proposed a three-dimensional randomly cross-linked network for the structure of metaphosphate glass (assumed a single phase), where the hydrogen bond involves essentially the P=O bond in P=O---OH–P linkages. Such bonds would be substantially stronger than the hydrogen bonds H–OH---OH–H in water. The nearest equivalent to the proposed bond would be the OH---O= bond in the acetic acid dimer. This bond has a stretching force constant of 39 N m^{-1}, more than twice the value of the same constant in the hydrogen bond in ice (18 N m^{-1}). Since the strong hydrogen bond in HPO_3 represents a bond linking two different cations (P and H) through oxygen, it represents a substantial contribution to $\Sigma n_j |V_i|$. So we have two "zero-point" factors acting against phase separation in the H_2O–P_2O_5 system, which is

*As the bond length for $Co(PO_3)_2$ is unavailable in the literature, we have taken the figure for the corresponding bond in the nearest equivalent structure ($CoNH_4P_3O_9$), for which a value is available.

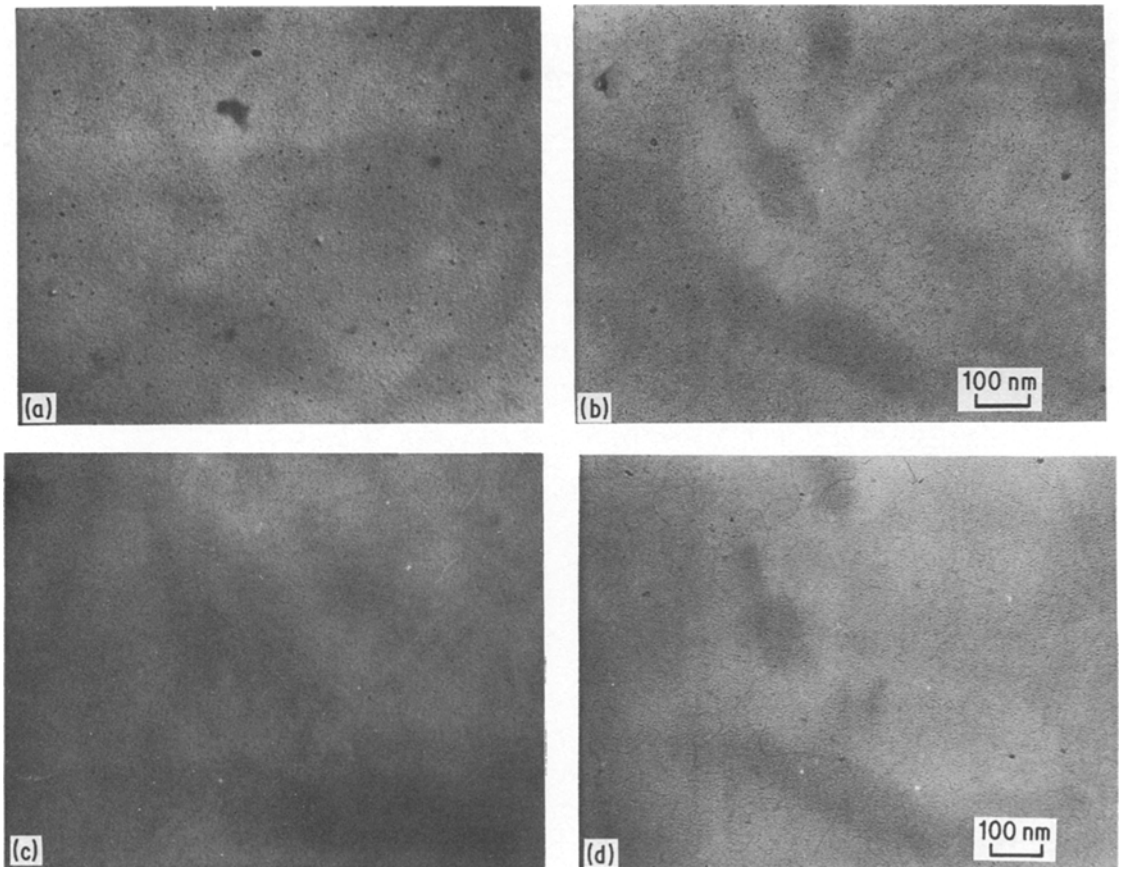

Figure 6 (a, b). Typical replica electron micrographs of Co–P–O glasses, which show that there is no evidence that immiscibility is present in Co–P–O glasses: (a) glass with composition of 7.6 mol % CoO, and (b) glass with composition of 20 mol % CoO. (c, d). Typical replica electron micrographs of Co–P–O glasses, which show that there is no evidence that immiscibility is present in Co–P–O glasses: (c) glass with composition of 35 mol % CoO, and (d) glass with composition of 54 mol % CoO.

possibly contrary to the indications of the ultrasonic experiments in the case of the water-rich glasses. The conclusion must be the same as in the case of Co–P–O glasses, i.e. that the phase structure of the melt is determined by the vibrational energy and entropy of the melt: for as argued at the beginning of this section, the vibrational term in Equation 14 tends to oppose any effect of the zero-point energy term.

References

1. R. SHAW and D. UHLMANN, *J. Non-Cryst. Solids* **5** (1971) 237.
2. W. VOGEL, *Glass Technol.* **1** (1966) 15.
3. W. VOGEL, W. SCHMIDT and L. HORN, *Silikattechn* **4** (1972) 112.
4. W. VOGEL, W. SCHMIDT and L. HORN, *Z. Chem.* **9** (1969) 401.
5. W.VOGEL, "Struktur und Kristallisation der Gläser" (VEB – Deutscher Verlay für Grundsoffindustrie, Leipzig, 1965).
6. P. F. JAMES, *J. Mater. Sci.* **10** (1975) 1802.
7. P. W. McMILLAN, "Glass Ceramics", 2nd edn. (Academic Press, London, 1979) p. 40.
8. A. A. HIGAZY and B. BRIDGE, *J. Non-Cryst. Solids* **72** (1985) 81.
9. *Idem, J. Mater. Sci.* **20** (1985) 2345.
10. *Idem, Phys. Chem.* **26** (1985) 82.
11. N. D. PATEL, B. BRIDGE and D. N. WATERS, *ibid.* **24**, (5) (1983) 122.
12. H. RAWSON, "Inorganic Glass Forming Systems" (Academic Press, London, 1967) p. 160.
13. P. W. McMILLAN, "Glass Ceramics", 2nd edn (Academic Press, 1979) p. 76.
14. R. SHAW and D. UHLMANN, *J. Non-Cryst. Solids* **1** (1969) 474.
15. E. M. LEVIN, "Phase Diagrams in Material Science and Technology", edited by A. M. Alpper (Academic Press, London, 1970) p. 218.
16. E. M. LEVIN, "Phase Diagrams in Material Science and Technology", edited by A. M. Alpper (Academic Press, London, 1970) p. 227.
17. R. SHAW and D. UHLMANN, *J. Non-Cryst. Solids* **5** (1971) 237.

18. Z. HASHIN, *J. Appl. Mech.* **29** (1962) 143.
19. Z. HASHIN and S. SHTRIKMAN, *J. Mech. Phys. Solids* **11** (1963) 127.
20. R. C. ROSSI, *J. Amer. Ceram. Soc.* **51** (1968) 433.
21. S. POPVIES, *Bull. Amer. Ceram. Soc.* **48** (1969) 1060.
22. C. M. SAYERS and R. L. SMITH, *J. Phys. D.* **16** (1983) 1189.
23. C. M. SAYERS and C. E. TAIT, *Ultrasonics* (1984) 57.
24. T. L. COTTRELL, "The Strengths of Chemical Bonds" (Butterworths, London, 1954) p.270.
25. B. BRIDGE, N. D. PATEL and D. N. WATERS, *Phys. Status Solidi (a)* **77** (1985) 655.
26. R. MASSE, A. DURIF and J. GUITEL, *Z. Kristallogr.* **BD141** (1975) 113.
27. L. V. TANANAEV and B. F. DZURINSKII, *Daki Chem.* **187** (1969) 615.
28. N. KRISHNANOCHEVI and C. CALVO, *Acta Crystallogr.* **B28** (1972) 2883.
29. N. C. TOOMBS and N. P. ROOKSBY, *Nature* **165** (1950) 442.
30. S. GREENWALD and J. S. SMART, *ibid.* **166** (1950) 523.
31. N. C. TOOMBS and H. P. ROOKSBY, *Phys. Rev.* **82** (1951) 113.
32. G. HAMPSON and A. STOSIK, *J. Amer. Chem. Soc.* **60** (1938) 1814.
33. G. A. SAUNDERS, private communication (1984).

Received 1 August 1984
and accepted 28 January 1985